Journal of ELECTRONIC MATERIALS, Vol. 32, No. 1, 2003 *Regular Issue Paper*

Electroless Cu Deposition Process on TiN for ULSI Interconnect Fabrication via Pd/Sn Colloid Activation

H.P. FONG,[1] Y. WU,[1] Y.Y. WANG,[1] and C.C. WAN[1,2]

1.—Department of Chemical Engineering, National Hsing-Hua University, Hsinchu, Taiwan.
2.—E-mail: ccwan@mx.nthu.edu.tw

In this study, (100)-orientation silicon wafer coated with TiN barrier is catalyzed by a Pd/Sn colloid, which serves as an activator for electroless copper deposition. After activation, electroless deposition of Cu occurs on the catalytic surface. The coverage of the Cu deposit reaches 100% and the adsorptive amount of Pd is greatly increased by the conditioning process. The correlation between deposition rate, resistivity, morphology, crystal structure, and composition of the deposit when varying the temperature of the plating bath is discussed. The deposition rate of Cu is monitored by both the electrochemical method and the profilometer (α-step), while the other properties of the deposit are measured by four-point probe, scanning electron microscopy (SEM), x-ray diffraction (XRD), and Auger electron microscopy (AES). Deposition at 70°C is favorable due to the higher deposition rate, lower resistivity, less impurities, and more preferred orientation in the crystal structure than that at lower temperature. Problems regarding adhesion and high resistivity can be greatly mitigated via 400°C thermal annealing. The resistivity of Cu can be reduced to 2.2 $\mu\Omega$cm. Moreover, trenches of 1 μm and 0.25 μm on patterned wafer have been successfully filled by electroless deposition of Cu with the aid of surfactant C12.

Key words: Electroless, Cu, Pd, colloid, ULSI

INTRODUCTION

Aluminum and its alloys are the most frequently used materials for interconnection in conventional ultralarge-scale integration (ULSI) fabrication. However, the application of Al encounters resistance-capacitance (RC) delay and electromigration problems when the critical dimension shrinks to submicron. Copper replaces Al to become the most feasible interconnect material due to its low resistivity and excellent electromigration resistance.[1] In addition, the development of chemical-mechanical polishing (CMP) slurry and dual damascence process enhances the feasibility of Cu interconnection.[2]

IBM claimed the first reliable construction of a Cu wiring structure by virtue of electrochemical deposition in 1997.[3] The electrochemical method is capable of forming reliable and superior Cu wiring structure with low expense, compared to that formed by the physical vapor deposition (PVD) or chemical vapor deposition (CVD) technique. Dubin et al.[4] deposited Ti as a barrier layer atop patterned wafer and then evaporated Pd or Au to catalyze the surface, which successfully triggered the electroless deposition of Cu. Desilva et al.[5] compared the electroless deposition and CVD technique on ULSI applications and stated that electroless deposition is favored by virtue of its selectivity. They also proclaimed the formation of a Cu layer with resistivity equal to 2 $\mu\Omega$cm only. Zhao and Vasudev[6] proposed the replacement of the Pd/Au catalytic layer by evaporating a 10- to 20-nm Cu seed together with 10- to 25-nm Al as a protection layer to prevent the Cu seed from oxidation. The Al sacrificial layer is removed when dipping into the alkaline electroless deposition solution and the exposed Cu seed can serve as a catalyst for subsequent deposition of Cu. Dubin et al.[7,8] formed 25-nm Ti, 40-nm TiN, or 40-nm Ta as a barrier layer and sputtered Cu seed as an activation layer for subsequent electroless plating, which comprised TMAH as a pH adjuster. The concentration of each component was also optimized by correlating it

(Received July 10, 2002; accepted August 20, 2002)

with the deposition rate and resistivity. In addition, a wet activation process has been adopted by Hsu et al.[9,10] The process comprises sensitization by $SnCl_2$ solution and activation by $PdCl_2$ solution. The two-step pretreatment and the following electroless Cu deposition are implemented on barrier materials such as TiN or TaN. However, the best result appears when electroless Cu is applied on the top of the sputtered Cu seed.

Pd/Sn colloid provides a potential alternative to the two-step method to trigger electroless Cu deposition atop TiN, and the one-step Pd/Sn colloid has generally replaced the two-step method in the printed circuit board (PCB) industry.[11] Although Pd/Sn colloid is capable of catalyzing electroless deposition atop the bumpy epoxy resin surface of PCB, its catalytic ability on the smooth TiN barrier has not yet been proven. In this study, Pd/Sn colloid is adopted to catalyze the TiN surface due to the simpler process and lower cost in comparison with other dry activation processes. The electroless deposition of Cu after activation is also optimized. In addition, since there is little information in the literature about the addition of surfactant in the electroless deposition bath, three types of surfactants were also selected for study.

EXPERIMENTAL

A (100)-orientation blanket silicon wafer coated with 30–50 nm TiN barrier was dipped into Pd/Sn colloid solution for 2–10 min with and without the conditioning step of a commercial conditioner (Crimson 5110, Shipley Corp.). Pd/Sn colloid solution was prepared as follows. First, 100-g $SnCl_2$ and 50-mL HCl were dissolved into 150-mL DI water and then heated to 80°C until $SnCl_2$ was completely dissolved. Next, 2-g $PdCl_2$ and 10-mL HCl were dissolved into 50-mL deionized (DI) water and heated to 80°C. The above two solutions were mixed and stirred for 1 h at 80°C and another 1 h without heating. After activation by immersing the wafer in the Pd/Sn colloidal solution, electroless deposition of Cu was executed on the catalyzed TiN barrier layer. The plating bath comprised $CuSO_4 \cdot 5H_2O$ as a metal source, EDTA as a chelating agent, NaOH as a pH adjuster, HCHO as a reducing agent, and pyridine as a stabilizing agent, as listed in Table I. The effectiveness of the conditioning process was examined by the coverage of the Cu deposit, and the Pd/Sn ratio of the catalytic surface was measured by inductively coupled plasma atomic emission spectrometer (ICP-AES). Fifty percent HCl was used here to dissolve the adsorbed Pd/Sn colloid into aqueous solution before analysis. The deposition rate was monitored by both the electrochemical method and α-step, which measures the surface profiles across a prescribed length by scanning a mechanical stylus. Resistivity, morphology, crystal structure, and composition of the deposit were measured by four-point probe, scanning electron microscopy (SEM), x-ray diffraction (XRD), and Auger electron spectroscopy (AES), respectively. In addition, a peel test was used to evaluate the adhesion strength of the deposit. The annealing process and the addition of surfactant were tried in order to enhance the adhesion of the deposit. The effectiveness of several surfactants was evaluated by measuring their contact angle. Based on the information obtained, an optimized process to fill 1- and 0.25-μm trenches was designed.

Table I. Composition of Electroless Deposition Bath for Cu

Component	Concentration	Function
$CuSO_4 \cdot 5H_2O$	12.5 (g/L)	Source of deposit
EDTA	37.5 (g/L)	Chelating agent
NaOH	14.5 (g/L)	PH adjuster
HCHO	5 (ml/L)	Reducing agent
C_5H_5N (pyridine)	100 (ppm)	Stabilizing agent

RESULTS AND DISCUSSION

The Pd/Sn colloid activation solution consists of 10 g/L $PdCl_2$, 500 g/L $SnCl_2$, and 300 mL/L HCl, which is 10–20 times more concentrated than that generally used in the PCB industry.[11] However, it is obviously still not enough for a smooth TiN surface to adsorb the required amount for subsequent deposition of Cu, as shown in Table II. Although the increase in temperature and that in immersion time can both enhance the Cu deposit coverage atop the blanket wafer, further improvement is necessary. Crimson 5110 is a widely used conditioner in the PCB industry, which acts to change the electrical charges on the glass fiber from negative to positive in order to make them more receptive to the negatively charged catalyst particles. This conditioner usually contains hydrophilic functional groups and hydrophobic carbon long chains. Theoretically, adhesion of the positively charged conditioner on TiN can greatly increase the adsorbed amount of negatively charged Pd/Sn colloid, thereby improving the coverage of Cu.[12] It was found that the coverage problem of the deposit is largely resolved via 10-min activation of Pd/Sn colloid at 60°C after conditioning by Crimson 5110 for 10 min at 45°C, as illustrated in Table II. The change after activation can also be witnessed by the color of the substrate, turning from TiN's golden shade to black-brown, representing

Table II. Coverage of Electroless Cu Deposit after Pd/Sn Colloid Activation with or without Conditioning Pretreatment

	Temperature		
Activation Time	20°C	40°C	60°C
2 min	0	0	0
5 min	0	0	2/10
10 min	0	1/10	5/10
2 min (after conditioning)	0	0	3/10
5 min (after conditioning)	0	1/10	5/10
10 min (after conditioning)	0	3/10	10/10

Table III. ICP Result of the Pd/Sn Contents per Gram of the Solution after Various Processes

Processes	Activation without Conditioning	Activation after Conditioning	Electroless Deposition after Conditioning and Activation
Pd contents ($\times 10^{-6}$ g)	0.07	1.02	0.914
Sn contents ($\times 10^{-6}$ g)	0.397	1.82	0.062

abundant Pd on the surface. Further evidence can be obtained by ICP, as listed in Table III. The adsorbed Pd and Sn after activation without conditioning are 7×10^{-8} g cm^{-2} and 3.97×10^{-7} g cm^{-2}, respectively. However, applying the conditioning process greatly increases the adsorbed amount of each to 1.02×10^{-6} g cm^{-2} and 1.82×10^{-6} g cm^{-2}, about 15 times and 4.5 times the original amount, respectively. In addition, the ratio of Pd/Sn is also increased from 1:5.25 to 1:1.8, which represents a marked enhancement on catalytic ability. This is due to the unique structure of the Pd/Sn colloid, in which the Pd/Sn alloy is located at the center and surrounded by inner-shell Sn^{2+} and outer-shell Cl^- ions. Osaka et al.[13] also mentioned this phenomenon when applying the Pd/Sn colloid to catalyze epoxy resin. The residual amount of Pd and Sn after deposition of Cu is also examined by ICP, which shows that 9.14×10^{-7} g cm^{-2} Pd and 6.2×10^{-8} g cm^{-2} Sn still exist on the substrate. The dramatic decline of the Sn content may result from the dissolution of Sn^{2+} and the formation of $Sn(OH)_2$ under the basic environment of plating bath.[14]

Figure 1 illustrates the polarization curve of electroless Cu deposition at 30°C and 70°C, respectively. An apparent shift of the curve is observed, which reveals that a faster deposition rate can be obtained at elevated temperature. Shacham-Diamand[15] proposed a mechanism for electroless deposition of Cu, which states that three main reactions are observed in the polarization curve:

$$[Cu(EDTA)]^{2-} + 2e \rightarrow Cu + (EDTA)^{4-} \qquad E = -0.466 \text{ versus SCE}$$

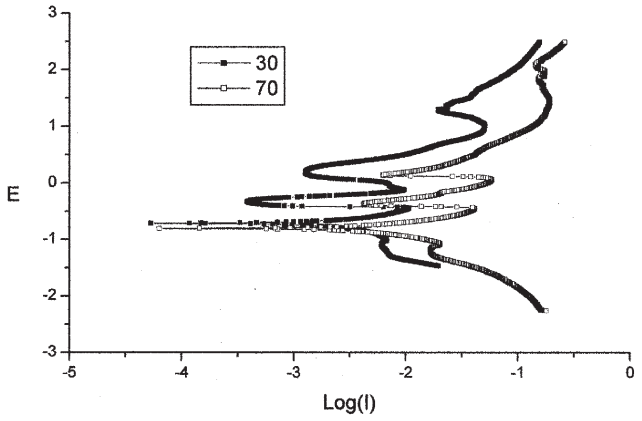

Fig. 1. Polarization curve of electroless deposition of Cu under 30°C and 70°C, respectively.

$$HCHO + 3OH^- \rightarrow HCOO^- + 2H_2O + 2e \qquad E = -1.169 \text{ versus SCE}$$

$$2H^+ + 2e \rightarrow H_2 \qquad E = -0.242 \text{ versus SCE}$$

The above three half-reactions can be observed in Fig. 1, regardless of the temperature. Based on the Tafel equation, the exchange current can be calculated by extrapolating the anodic and cathodic polarization curve to reach an intersection. The deposition rate can also be found by applying Faraday's law. Table IV lists the calculated result of the exchange current and the deposition rate of Cu. The density of Cu used in the calculation was 8.97 g/cm^3. The exchange current and the deposition rate increase with increasing temperature. Additionally, weight analysis assisted by the α-step is also applied to ensure the estimation of the electrochemical method. Table V lists the weight difference before and after the deposition under various temperatures, and the related deposition rate evaluated from the deposit thickness is measured by the α-step. The deposition rate estimated by the electrochemical method is higher than that evaluated by the α-step to some degree. This finding may result from the lack of activation step in the electrochemical method, which uses a Pt electrode to measure the polarization curve. Direct electric current supplied from external power also eliminates the duration time needed in the real situation. The rate equation of spontaneous electroless Cu deposition can be expressed as follows:

$$R = K[Cu^{2+}]^a[OH^-]^b[HCHO]^c[EDTA]^d \exp(-\Delta E/RT) \quad (1)$$

The above equation can be rewritten as if the concentration of each component can be regarded as constant:

$$R = A \exp(-\Delta E/RT) \quad (2)$$

where $A = K[Cu^{2+}]^a[OH^-]^b[HCHO]^c[EDTA]^d$

The activation energy ΔE and the pre-exponential factor A can be estimated by the curve B in Fig. 2. The Arrhenius-type equation can now be written as

$$R = 2.22 \times 10^7 \exp(53{,}350/RT) \quad (3)$$

where $\Delta E = 53.35$ kJ/mol and $A = 2.22 \times 10^7$ μm/min

Dubin and Shcham-Diamond[7] proposed a study of the kinetics of electroless deposition of Cu in which a similar activation energy value about 60.9 kJ/mol

Table IV. The Exchange Current and Deposition Rate Calculated from the Polarization Curve under Various Temperatures

Temperature	Exchange Current I_0 (A/cm^2)	Deposition Rate in Weight (g/h·cm^2)	Deposition Rate in Thickness (μm/min·cm^2)
30°C	0.0015	0.0018	0.034
40°C	0.0022	0.0026	0.048
50°C	0.0039	0.0046	0.087
60°C	0.0067	0.0079	0.140
70°C	0.0089	0.0105	0.196

Table V. Comparison between the Estimated Deposition Rate by Electrochemical Method and Weight Analysis Assisted by α-Step

Temperature (°C)	Weight Difference before and after 10 min Deposition (g)	Deposition Rate Estimated by I_0 (μm/min)	Deposition Rate Estimated by α-Step (μm/min)
30	0.00020	0.022	0.013
40	0.00034	0.038	0.035
50	0.00062	0.069	0.047
60	0.00108	0.121	0.086
70	0.00167	0.186	0.175

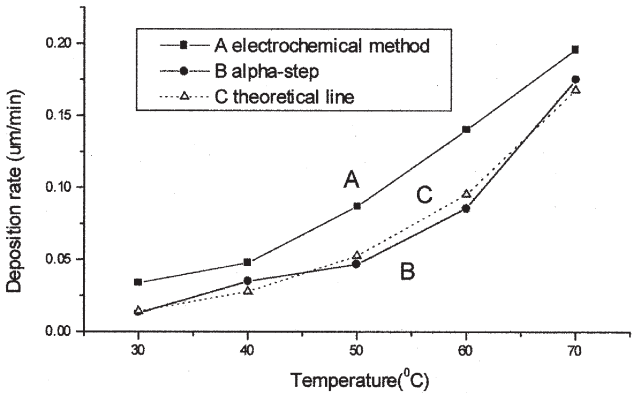

Fig. 2. Correlation between deposition rate and temperature schematized *via* two different methods.

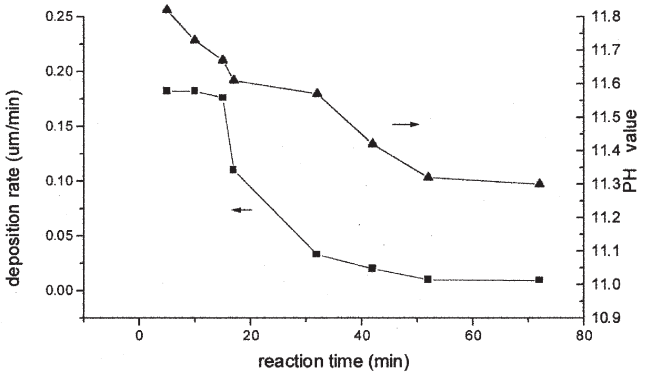

Fig. 3. The relationship between deposition rate, pH value, and reaction time in electroless deposition of Cu.

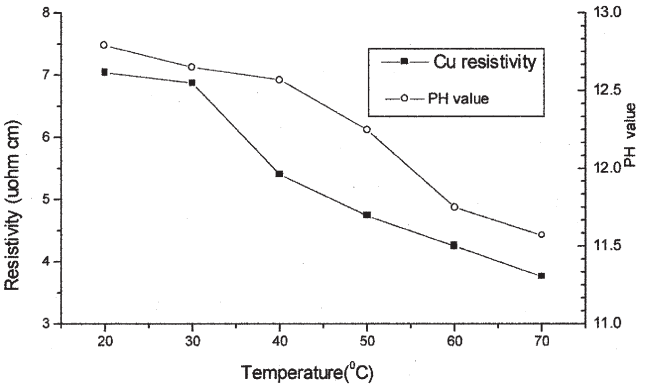

Fig. 4. Resistivity and pH vary with the temperature.

is reported. The rate response to temperature by Eq. 3 is shown in Fig. 2 together with the results by the electrochemical method and α-step approach. The relationship between deposition rate, pH value, and reaction time is shown in Fig. 3. The consumption of OH^- continues with electroless deposition; thereby, pH gradually decreases with time. However, the pH has a large influence on the half-wave potential of the oxidation of HCHO. When the pH changes from 14 to 0, the half-wave potential of HCHO oxidation also changes from −1.072 V to −0.059 V. Thus, the reaction rate gradually decreases with time and approaches zero when the reaction time exceeds 50 min, as shown in Fig. 3. Although raising the pH can increase the efficiency of deposition, excessive OH^- leads to the generation of $Cu(OH)_2$, which makes the plating bath unstable. The appropriate pH of the plating bath should range from 11.5 to 12.5, as suggested by the study of Dubin and Shcham-Diamond.[7]

Figure 4 illustrates that both the pH of the plating solution and the resistivity of the deposit gradually decrease with increasing temperature. The existence of other impurities usually results in the elevation of resistivity of the deposit. The results from ICP and AES analysis both support our hypothesis. The mixing solution of H_2SO_4 and H_2O_2 was applied to dissolve the Cu deposit into aqueous solution for measurement of ICP. Results show that the Cu content in each gram of the deposit equals 0.881 g at

30°C and 0.953 g at 70°C, respectively. In addition, AES was applied to analyze the impurities of the Cu layer deposited at 70°C, which illustrates the existence of C, O, and S in the deposit. The C and S atom should come from the chelating agent EDTA and SO_4^{2-} in plating solution, while the O atom may come from the OH^- in solution or the oxidation of Cu when exposed in the air. Moreover, the lowest resistivity of the Cu deposit is about 3.53 μΩcm, which is still much higher than the theoretical 1.7 μΩcm and the 2.5 μΩcm reported by Hsu et al.[10] Further improvement of the plating bath composition or post treatment of the deposit is required. Different morphologies of the Cu deposit due to temperature variation were monitored by SEM, as shown in Figure 5, together with the cross section of the deposit. The grain size of Cu deposited at 30°C ranges from 0.5 to 0.7 μm, smaller than that formed at 70°C, which equals about 0.1 μm only. The surface is rougher when Cu is deposited at lower temperature. The deposition rate of Cu can also be estimated from the thickness of the Cu layer. The estimated deposition rates for Cu at 30°C and 70°C are 0.035 μm/min and 0.175 μm/min, respectively, similar to that calculated by electrochemical method and α-step measurement. Consequently, deposition at low temperature is unfavorable due to its lower deposition rate, higher resistivity, and larger content of impurities.

In addition to resistivity, adhesion is another essential factor in evaluating the feasibility of interconnection via electroless deposition. A peel test was introduced to measure the adhesion between Cu deposit and the underlying TiN/Si substrate. However, about 70% of the as-deposited Cu was peeled off during the test, which shows that the adhesion of the deposit is insufficient. Three different methods were used for improvement. First, constant mechanical force was applied to roughen the TiN surface before activation. However, the effect of surface roughness by mechanical force was not apparent. The adhesive area of Cu only slightly increases to about 80%. Second, we tried to use chemicals to moderately etch

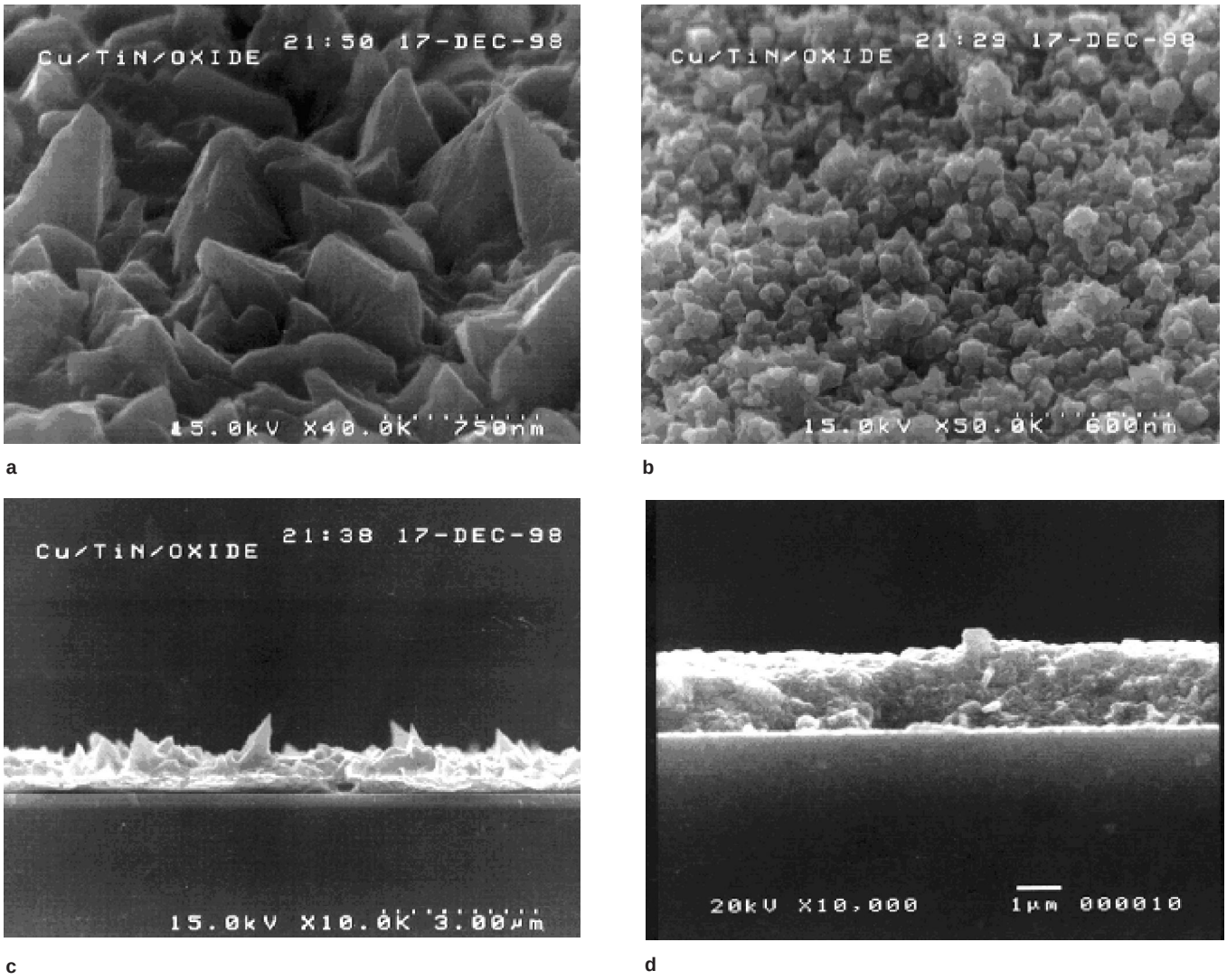

Fig. 5. The crystal morphology of Cu deposit *via* electroless deposition under (a) 30°C and (b) 70°C, and the cross section of the deposit under (c) 30°C and (d) 70°C.

the TiN surface, such as 2% HF and 10% NaOH. However, etching produced no obvious improvement on the adhesion of Cu; 2% HF even corroded the TiN in an excessive rate equal to about 17 nm/min. The last method applies thermal treatment on the as-deposited Cu. Figure 6 shows the peel test result of Cu deposit after 400°C annealing. The adhesion of Cu can be greatly improved to pass the peel test by 400°C annealing for 20 min. This finding may result from a stronger binding force between Cu and TiN substrate due to their interdiffusion. Similar results have been reported by Hsu et al.[9] The crystal structure and the resistivity of the deposit also change after the thermal annealing process. Figure 7 shows the crystal morphology before and after the thermal process. Original fine Cu grains rearrange and grow into larger grains during annealing, which implies that the grain boundary of the deposit is reduced and thus enhances the growth of the preferable (111) structure. The XRD result corresponds to the above observation, in which the ratio of plane (111) to (200) increases to 3.10, higher than 2.57 of as-deposited Cu. Additionally, the decline of resistivity after annealing also corresponds to the variation in crystal structure, as shown in Fig. 8. The resistivity of Cu after 400°C annealing for 50–60 min can be reduced to about 2.2 $\mu\Omega$cm only, much lower than that of as-deposited Cu.

Since the activation process by Pd/Sn colloid is necessary for the subsequent electroless deposition process, the wettability of activation solution is essential for the submicron trench filling. The wettability of solution can be estimated via the measurement of contact angle. The definition of contact angle can be expressed as follows:

$$\cos\theta = \gamma_{Se} - \gamma_{SL}/\gamma_L \quad (4)$$

where γ_{Se} represents the surface tension between the substrate and air, γ_{SL} represents the surface tension between the substrate and liquid, and γ_L stands for the surface tension of liquid.

The force γ_{Se} is to spread the liquid drop on the solid substrate and is usually a constant for a specific solid substrate. Adding a surfactant into the solution can help to decrease both γ_{SL} and γ_L, thereby decreasing the contact angle and enhancing the wettability of the solution. Surfactants selected in this study can be categorized into three types. The first type such as PEG and hexane has commonly been used in conventional electrodeposition of Cu. The second type belongs to the Aerosol series, which contains the SO_3Na functional group and the diester structure, inclusive of Aerosol MA, Aerosol OT, and Aerosol 22. The third type is $C_{12}H_{25}C_6H_4SO_3Na$ (C12), which is designed for acidic solution. The contact angle of commercially available surfactant (32C) is also measured for comparison. Information on all selected surfactants is listed in Table VI, including their chemical formula and molecular weight.

It has been found that the contact angle between TiN and conditioner Crimson 5110 is only 17°; however, the contact angle between TiN and the activation solution is 47°, much greater than that of a commonly wetted surface. C12 was then selected to test

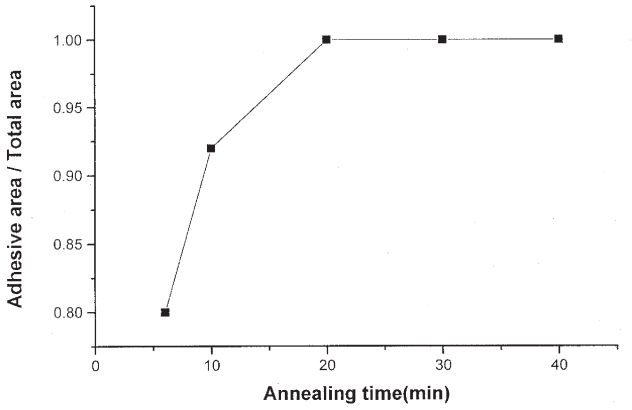

Fig. 6. The correlation between annealing time and the improvement of adhesion.

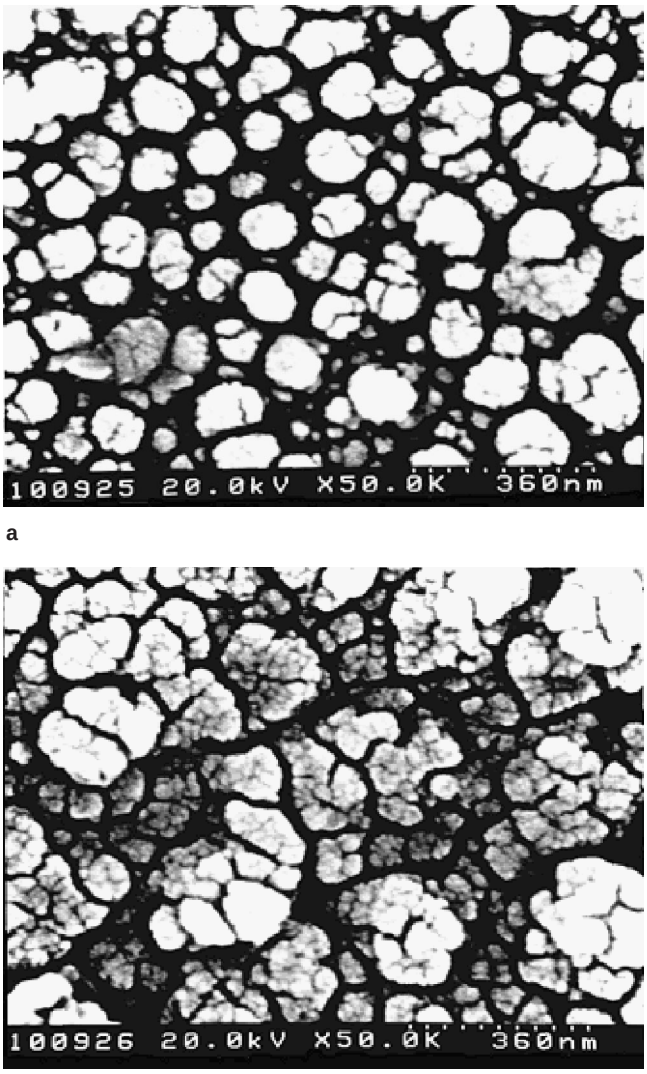

Fig. 7. Crystal morphology of Cu (a) before and (b) after 400°C annealing for 20 min.

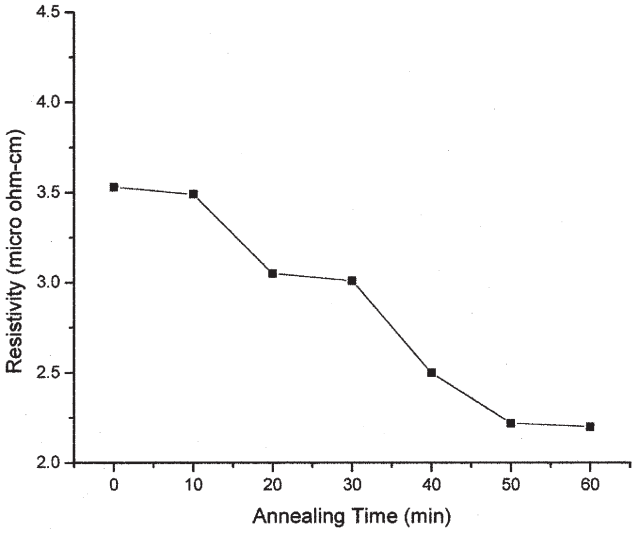

Fig. 8. The relationship between annealing time and resistance.

its effectiveness to enhance wettability in a highly acidic activator containing abundant HCl. The result is depicted in Fig. 9, which shows an obvious improvement when the C12 concentration is higher than 0.5 g/L. However, it is known that micelle of surfactant may form when the surfactant concentration is too high. Too much surfactant could hinder solution wetting and result in undesirable voids inside the deposit. Two tangent lines can be drawn in Fig. 9 to obtain the critical micelle concentration. In this case, the critical micelle concentration is about 0.6–0.7 g/L. In addition, the contact angle measurement between the catalytic surface and plating solution of Cu is also required to ensure reliable trench filling.

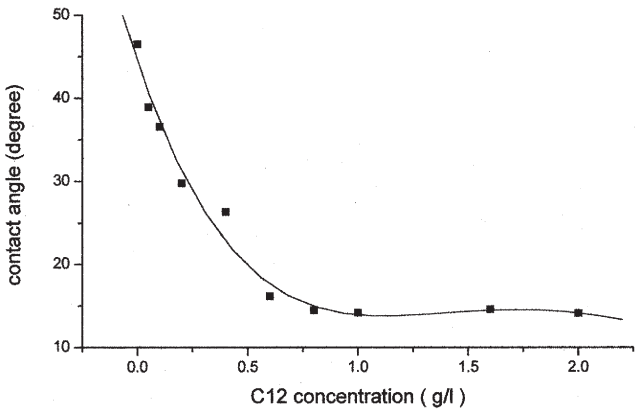

Fig. 9. Contact angle varies with C12 concentration in Pd/Sn colloid activation.

However, the contact angle of the plating solution is 33°, which indicates that improvement of wettability is also necessary by adding surfactant. Figure 10 depicts the correlation between the contact angle and concentration of all selected surfactants. Almost all surfactants are capable of decreasing the contact angle to 20°; however, only Aerosol MA, C12, and 32C exhibit excellent wettability by reducing the contact angle below 15°. In particular, C12 can reduce the contact angle to 12°. Consequently, C12 was chosen as the surfactant. The concentration is slightly less than its critical micelle concentration, which is about 0.2–0.3 g/L. Trench filling of the 1 μm and 0.25 μm pattern wafer by electroless Cu was executed with or without the addition of surfactant C12, as shown in Fig. 11. A void or overhang situation is greatly enhanced by the addition of C12. Both the 1 μm and

Table VI. Category of Selected Three Types of Surfactant

Type	Surfactant	Chemical Formula	MW
1	Polyethylene glycol	$-(CH_2CH_2)-$ OH	2600–3800
1	Hexane	$H_3C-(CH_2)_4-CH_3$	86.17
2	Aerosol OT	$CH_2COOC_8H_{17}$ | $CHCOOC_8H_{17}$ | SO_3Na	444.22
2	Aerosol MA	$CH_2COOC_6H_{13}$ | $CHCOOC_6H_{13}$ | SO_3Na	388.45
2	Aerosol 22	CH_2COONa | $CHCOONa$ | $CH_2CONC_{18}H_{37}$ | $CHCOONa$ | SO_3Na	653.65
3	Sodium dodecylbenzenesulfonate (C12)	$C_{12}H_{25}$–C$_6$H$_4$–SO_3Na	348.19
3	32C	Unknown	Unknown

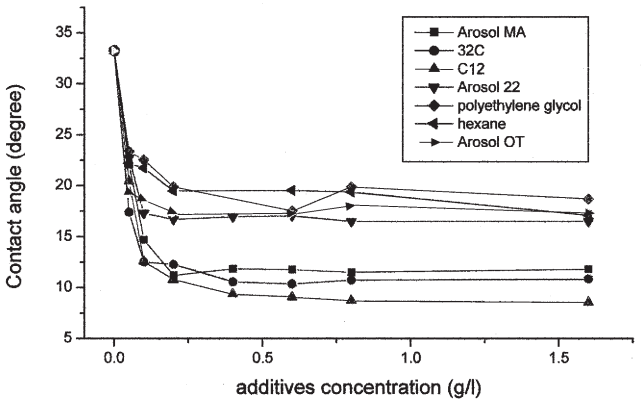

Fig. 10. The comparison of contact angles among different surfactants adding into the plating bath for electroless Cu deposition.

0.25 μm trenches can be successfully filled by electrolessly deposited Cu.

CONCLUSIONS

Although electroless deposition of Cu cannot be executed on TiN/Si directly, pretreatment by a Pd/Sn colloid activator successfully catalyzes the surface. The coverage of the Cu deposit can reach 100% by surface conditioning at 45°C followed by activation at 60°C before deposition. The amount of Pd adsorbed and the Pd/Sn ratio both apparently increase after the conditioning process, thereby improving the coverage of Cu. The deposition rate, resistivity, composition, and crystal structure are measured and correlated at various temperatures. Consequently, a practical electroless deposition process for Cu can be designed based on the above information. Deposition at 70°C is favorable due to its higher deposition rate, lower resistivity, fewer impurities, and more preferred orientation (111) in crystal structure than at lower temperature. The deposition rate at 70°C is about 0.175 μm/min and the resistivity of as-deposited Cu is 3.53 μΩcm. In addition, problems regarding poor adhesion and high resistivity of the electroless Cu can be greatly mitigated via 400°C annealing. The resistivity of Cu can be reduced to 2.2 μΩcm, much lower than that of as-deposited Cu. Moreover, the contact angle of sev-

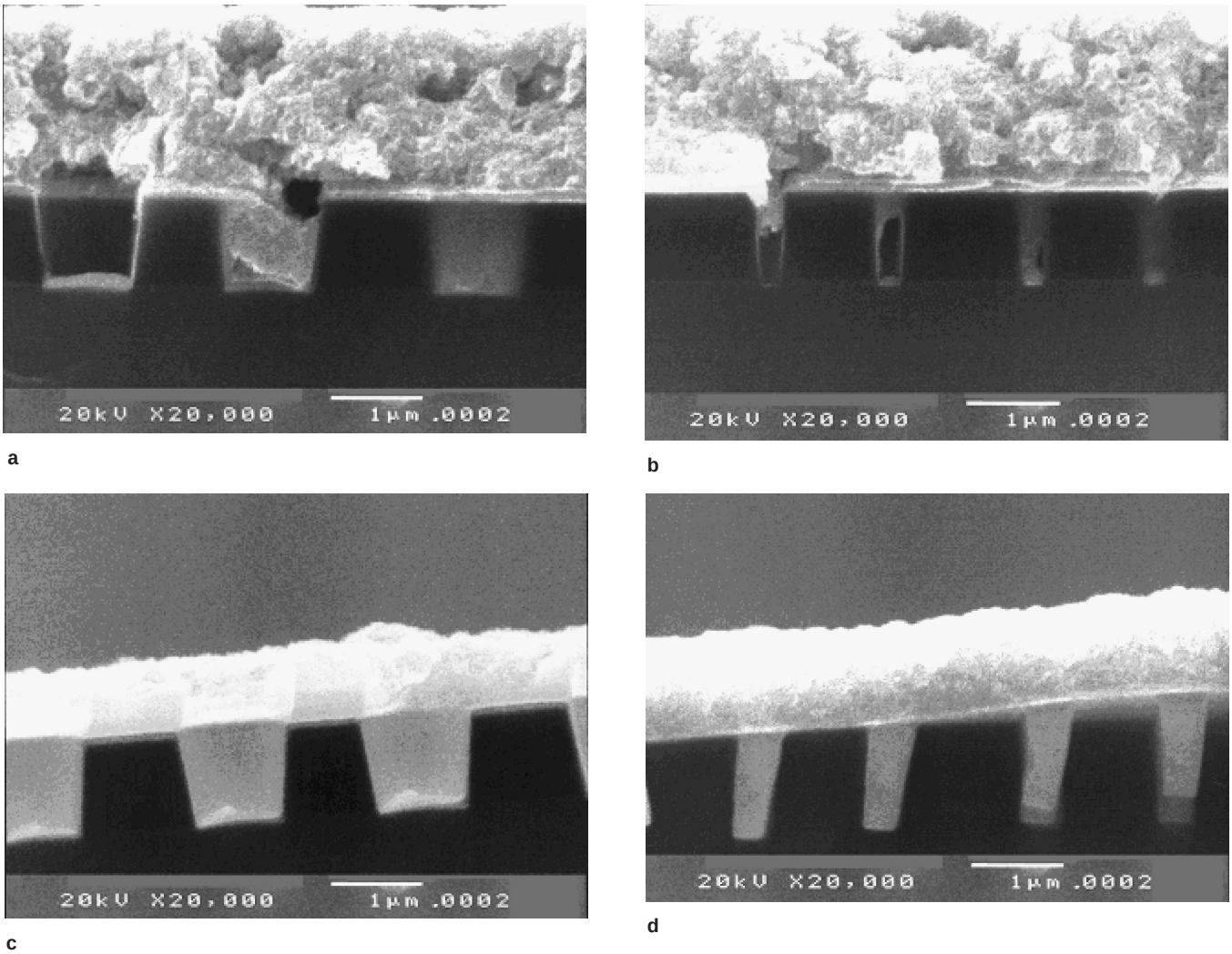

Fig. 11. Trench filling of (a) 1 μm and (b) 0.25 μm pattern without any surfactant. Trench filling of (c) 1 μm and (d) 0.25 μm pattern with the addition of C12.

eral surfactants has been measured to evaluate their promotion on wettability for both the activation solution and Cu plating bath. C12 is found to be the most favorable choice among tested additives.

ACKNOWLEDGEMENT

Support for this work was obtained from the National Science Council of Taiwan.

REFERENCES

1. J.D. Plummer, M.D. Deal, and P.B. Griffin, *Silicon VLSI Technology* (Englewood Cliffs, NJ: Prentice-Hall, Inc., 2000), pp. 570–572.
2. P.C. Andricacos, *Interface* 8, 32 (1999).
3. P.C. Andricacos, C. Uzoh, J.O. Dukovic, J. Horkans, and H. Deligianni, *IBM J. Res. Develop.* 42, 567 (1998).
4. V.M. Dubin, C.H. Ting, and R. Cheung, *VMIC Conf.* (1997).
5. M.J. Desilva, V. Dubin, and Y. Shcham-Diamand, *J. Mater. Res.* 11, 607 (1996).
6. B. Zhao and P.K. Vasudev, *J. Mater. Res.* 11, 179 (1996).
7. V.M. Dubin and Y. Shcham-Diamand, *J. Electrochem. Soc.* 144, 898 (1997).
8. V.M. Dubin, *J. Electrochem. Soc.* 139, 633 (1992).
9. H.H. Hsu, K.H. Lin, S.J. Lin, and J.W. Yeh, *J. Electrochem. Soc.* 148, C47 (2001).
10. H.H. Hsu, C.W. Ting, S.J. Lin, and J.W. Yeh, *J. Electrochem. Soc.* 149, C143 (2002).
11. E.D. D'Ottavio, U.S. patent 3,532,518 (1970); U.S. patent 3,650,913 (1972).
12. M.W. Jawitz, *Printed Circuit Board Materials Handbook* (New York, NY: McGraw-Hill Companies, Inc., 1997), pp. 23.1–23.5.
13. T. Osaka, H. Takematsu, and K Nihei, *J. Electrochem. Soc.* 148, C162 (1980).
14. C.S. Yang, C.C. Chen, Y.Y. Wang, and C.C. Wan, *J. Electrochem. Soc.* 143, 3521 (1996).
15. Y. Shcham-Diamand, V.M. Dubin, and M. Angyal, *Thin Solid Film* 262, 93 (1995).